Synthesis, Crystal Structure, and Magnetic Properties of Two Cyano-Bridged Bimetallic 4f−3d Arrays with One-Dimensional Chain and Two-Dimensional Brick Wall Molecular Structures

Hui-Zhong Kou, Song Gao,* and Xianglin Jin

State Key Laboratory of Rare Earth Materials Chemistry and Applications, PKU−HKU Joint Laboratory on Rare Earth Materials and Bioinorganic Chemistry, College of Chemistry and Molecular Engineering, Peking University, Beijing 100871, P. R. China

Received March 20, 2001

The design, synthesis, and structural and magnetic properties of the two new bimetallic complexes $[Sm(DMF)_4(H_2O)_2Cr(CN)_6]\cdot H_2O$ and $[Sm(DMF)_2(H_2O)_3Cr(CN)_6]\cdot H_2O$ (DMF = *N*,*N*-dimethylformamide) are presented. $[Sm(DMF)_4(H_2O)_2Cr(CN)_6]\cdot H_2O$ was prepared by the reaction between Sm^{3+} and $[Cr(CN)_6]^{3-}$ in a methanol−DMF solution, while $[Sm(DMF)_2(H_2O)_3Cr(CN)_6]\cdot H_2O$ was prepared by the reaction between Sm^{3+}, DMF, and $[Cr(CN)_6]^{3-}$ in the molar ratio of 1:2:1 in H_2O. $[Sm(DMF)_4(H_2O)_2Cr(CN)_6]\cdot H_2O$ crystallizes in the monoclinic space group of $P2(1)/c$ with $a = 13.161(3)$ Å, $b = 12.928(3)$ Å, $c = 19.174(4)$ Å, $\beta = 109.82(3)°$, and $Z = 4$, while $[Sm(DMF)_2(H_2O)_3Cr(CN)_6]\cdot H_2O$ is in the triclinic space group $P\bar{1}$ with $a = 7.7535(1)$ Å, $b = 9.4307(3)$ Å, $c = 16.2905(5)$ Å, $\alpha = 94.1590(14)°$, $\beta = 100.0597(18)°$, $\gamma = 100.9154(18)°$, and $Z = 2$. The structure of $[Sm(DMF)_4(H_2O)_2Cr(CN)_6]\cdot H_2O$ possesses a cyano-bridged one-dimensional (1D) zigzag chain structure with alternating $Sm(DMF)_4(H_2O)_2$ and $Cr(CN)_6$ moieties. $[Sm(DMF)_2(H_2O)_3Cr(CN)_6]\cdot H_2O$ consists of cyano-bridged neutral brick wall-like layers in which each $[Cr(CN)_6]^{3-}$ unit uses three cyanide groups in the meridional arrangement to connect with three $[Sm(DMF)_2(H_2O)_3]^{3+}$ units. Each $[Sm(DMF)_2(H_2O)_3]^{3+}$ unit, in turn, links three $[Cr(CN)_6]^{3-}$, generating a flat brick wall-like structure. Magnetic studies on $[Sm(DMF)_2(H_2O)_3Cr(CN)_6]\cdot H_2O$ showed a magnetic-phase transition temperature below 4.2 K and a coercive field of 100 Oe at 1.85 K, while no long-range magnetic ordering was observed in the 1D complex $[Sm(DMF)_4(H_2O)_2Cr(CN)_6]\cdot H_2O$.

Introduction

Recently, there has been considerable interest in lanthanide(III) hexacyanoferrates and the analogous hexacyanocobaltate as well as hexacyanochromiumate complexes because of their potential as catalytic and semiconductive materials.[1] In 1976, a series of cyano-bridged three-dimensional (3D) rare-earth hexacyanometalates(III) $LnM(CN)_6\cdot nH_2O$ (M = Fe or Cr, $n = 4$ or 5) were crystallized and subjected to single-crystal X-ray and magnetic susceptibility measurements.[2] Ferrimagnetic ordering was observed for $LnCr^{III}(CN)_6\cdot nH_2O$ (Ln = Nd, Sm, Gd, Tb, Dy, Ho, Er, and Tm), and $TbCr(CN)_6\cdot 4H_2O$ has the highest magnetic-phase transition temperature of 11.7 K. Incorporation of organic ligands into the 3D solids would produce 4f−3d species with rich and interesting molecular structures.[3−7] This strategy has also been successfully employed for the preparation of hybrid 3d Prussian blue analogues.[8] Using DMF as a ligand, a cyano-bridged 4f−3d dimer $[Sm(DMF)_4(H_2O)_4Fe(CN)_6]\cdot H_2O$ was obtained, which can be described as a variation of 3D $SmFe(CN)_6\cdot 4H_2O$.[4] Similar cyano-bridged binuclear $[Ln(DMF)_4(H_2O)_3Fe(CN)_6]\cdot H_2O$ (Ln = lanthanide

(1) Traversa, E.; Nunziante, P.; Sakamoto, M.; Watanabe, K.; Sadaoka, Y.; Sakai, Y. *Chem. Lett.* **1995**, 189. Sadaska, Y.; Traversa, E.; Sakamoto, M. *Chem. Lett.* **1996**, 1747.

(2) Hulliger, F.; Landolt, M.; Vetsch, H. *J. Solid State Chem*. **1976**, *18*, 283.

(3) Gao, S.; Ma, B.-Q.; Wang, Z.-M.; Yi, T.; Liao, C.-S.; Yan, C.-H.; Xu, G.-X. *Mol. Cryst. Liq. Cryst.* **1999**, *334*, 913. Garcia-Granda, S.; Morales, A. D.; Ruiz, E. R.; Bertran, J. F. *Acta Crystallogr*. **1996**, *C52*, 1679. Yi, T.; Gao, S.; Chen, X. W.; Yan, C. H.; Li, B. G. *Acta Crystallogr*. **1998**, *C54*, 41. Yan, B.; Chen, Z. *Helv. Chim. Acta* **2001**, *84*, 817. Yan, B.; Wang, H. D.; Chen, Z. D. *Inorg. Chem. Commun.* **2000**, *3*, 653.

(4) Kou, H.-Z.; Yang, G.-M.; Liao, D.-Z.; Cheng, P.; Jiang, Z.-H.; Yan, S.-P.; Huang, X.-Y.; Wang, G.-L. *J. Chem. Crystallogr*. **1998**, *28*, 303.

(5) (a) Kautz, J. A.; Mullica, D. F.; Cunningham, B. P.; Combs, R. A.; Farmer, J. M. *J. Mol. Struct*. **2000**, *523*, 175. (b) Mullica, D. F.; Farmer, J. M.; Cunningham, B. P.; Kautz, J. A. *J. Coord. Chem*. **2000**, *49*, 239. (c) Combs, R. A.; Farmer, J. M.; Kautz, J. A. *Acta Crystallogr*. **2000**, *C56*, 1420.

(6) (a) Knoeppel, D. W.; Shore, S. G. *Inorg. Chem.* **1996**, *35*, 1747. (b) Knoeppel, D. W.; Shore, S. G. *Inorg. Chem.* **1996**, *35*, 5328. (c) Knoeppel, D. W.; Liu, J.; Meyers, E. A.; Shore, S. G. *Inorg. Chem*. **1998**, *37*, 4828. (d) Du, B.; Meyers, E. A.; Shore, S. G. *Inorg. Chem*. **2000**, *39*, 4639.

(7) Ma, B.-Q.; Gao, S.; Su, G.; Xu, G.-X. *Angew. Chem., Int. Ed.* **2001**, *40*, 434.

(8) (a) Langenberg, K. V.; Batten, S. R.; Berry, K. J.; Hockless, D. C. R.; Moubaraki, B.; Murray, K. S. *Inorg. Chem*. **1997**, *36*, 5006. (b) El Fallah, M. S.; Rentschler, E.; Caneschi, A.; Sessoli, R.; Gatteschi, D. *Angew. Chem., Int. Ed. Engl*. **1996**, *35*, 1947. (c) Ferlay, S.; Mallah, T.; Vaissermann, J.; Bartolome, F.; Veillet, P.; Verdaguer, M. *J. Chem. Soc., Chem. Commun*. **1996**, 2481. (d) Colacio, E.; Dominguez-Vera, J. M.; Ghazi, M.; Kivekas, R.; Lloret, F.; Moreno, J. M.; Stoeckli-Evans, H. *Chem. Commun.* **1999**, 987. (e) Kou, H.-Z.; Gao, S.; Bu, W.-M.; Liao, D.-Z.; Ma, B.-Q.; Jiang, Z.-H.; Yan, S.-P.; Fan, Y.-G.; Wang, G.-L. *J. Chem. Soc., Dalton Trans*. **1999**, 2477. (f) Zhang, S.-W.; Fu, D.-G.; Sun, W.-Y.; Hu, Z.; Yu, K.-B.; Tang, W. X. *Inorg. Chem*. **2000**, *39*, 1142. (g) Smith, J. A.; Galan-Mascaros, J.-R.; Clerac, R.; Dunbar, K. R. *Chem. Commun*. **2000**, 1077. (h) Sra, A. K.; Andruh, M.; Kahn, O.; Golhen, S.; Ouahab, L.; Yakhmi, J. V. *Angew. Chem., Int. Ed.* **1999**, *38*, 2606. (i) Marvillers, A.; Parsons, S.; Riviere, E.; Audiere, J.-P.; Mallah, T. *Chem. Commun*. **1999**, 2217. (j) Mondal, N.; Saha, M. K.; Bag, B.; Mitra, S.; Gramlich, V.; Ribas, J.; El Fallah, M. S. *J. Chem. Soc., Dalton Trans*. **2000**, 1601. (k) Ohba, M.; Usuki, N.; Fukita, N.; Okawa, H. *Angew. Chem., Int. Ed.* **1999**, *38*, 1795.

10.1021/ic0103042 CCC: $20.00
Published on Web 10/09/2001

Table 1. Crystallographic Data for Complexes **2** and **3**

	2	**3**
formula	$C_{18}H_{34}CrN_{10}O_7Sm$	$C_{12}H_{22}CrN_8O_6Sm$
fw	704.90	576.73
λ/Å	0.710 73	0.710 73
space group	$P2_1/c$	$P\bar{1}$
a/Å	13.161(3)	7.7535(1)
b/Å	12.928(3)	9.4307(3)
c/Å	19.174(4)	16.2905(5)
α/deg	90	94.1590(14)
β/deg	109.82(3)	100.0597(18)
γ/deg	90	100.9154(18)
V/Å^3	3069.1(12)	1144.75(5)
Z	4	2
ρ_{calcd}/(g cm^{-3})	1.526	1.673
μ(Mo Kα)/mm^{-1}	2.298	3.055
reflns collected	10423	17175
independent reflns	5405	4015
data/restraints/params	5405/0/358	4015/0/286
R [$I > 2\sigma(I)$]	0.0372	0.0330
wR2 (all data)	0.0895	0.0828

ions except Sm and Nd) complexes and $[Pr(DMF)_4(H_2O)_3Cr(CN)_6]\cdot H_2O$ have been reported subsequently.[5] However, cyano-bridged two-dimensional (2D) 4f−3d assemblies have been rarely characterized so far, especially an ordering one.[7] We just communicated a 2D brick wall-like bimetallic complex $[Gd(DMF)_2(H_2O)_3Cr(CN)_6]\cdot H_2O$[9] (**1**) with long-range antiferromagnetic ordering below 3.5 K and a small coercive field of less than 10 Oe at 1.8 K. As an extension of this work, two bimetallic Sm−Cr complexes were synthesized and characterized, because the Sm^{3+} ion is anistropic and a magnet with a larger coercive field was expected. We report here the synthesis, structures, and magnetic investigations of $[Sm(DMF)_4(H_2O)_2Cr(CN)_6]\cdot H_2O$ (**2**) and $[Sm(DMF)_2(H_2O)_3Cr(CN)_6]\cdot H_2O$ (**3**).

Experimental Section

Elemental analyses of carbon, hydrogen, and nitrogen were carried out with an Elementar Vario EL. The infrared spectroscopy on KBr pellets was performed on a Magna-IR 750 spectrophotometer in the 4000−400 cm^{-1} region. Variable-temperature magnetic susceptibility, zero-field ac magnetic susceptibility measurements, and field dependence magnetization were performed on a Maglab System 2000 magnetometer. Effective magnetic moments were calculated by the equation $\mu_{eff} = 2.828(\chi_m T)^{1/2}$, where χ_m is the molar magnetic susceptibility. The experimental susceptibilities were corrected for the diamagnetism of the constituent atoms (Pascal's tables).

Syntheses. All of the chemicals and solvents used in the synthesis were reagent grade. The precursors $K_3[Cr(CN)_6]$ and $(Bu_4N)_3[Cr(CN)_6]$ were prepared by the literature methods.[10,11]

$[Sm(DMF)_4(H_2O)_2Cr(CN)_6]\cdot H_2O$ (2). To $SmCl_3\cdot 6H_2O$ (1 mmol) in DMF (5 mL) was added dropwise, with stirring, an equal molar amount of $(Bu_4N)_3[Cr(CN)_6]$ in absolute MeOH (5 mL). Slow evaporation of the resultant yellow mixture in the dark at room temperature gave well-shaped single crystals. Anal. Calcd (%) for $C_{18}H_{34}N_{10}O_7CrSm$ (704.90): C, 30.67; N, 19.87; H, 4.86. Found: C, 30.14; N, 19.94; H, 4.68. IR (cm^{-1}, KBr): $\nu_{C\equiv N}$ 2141, 2126, $\nu_{C=O}$ 1653.

$[Sm(DMF)_2(H_2O)_3Cr(CN)_6]\cdot H_2O$ (3). To an aqueous solution of $Sm(NO_3)_3\cdot 6H_2O$ (0.5 mmol) and DMF (1 mmol) was added $K_3[Cr(CN)_6]$ (0.5 mmol) in water (5 mL). The resultant yellow mixture was kept undisturbed in the dark at room temperature. After 1 week, large platelike yellow single crystals suitable for X-ray diffraction analysis were obtained. IR (cm^{-1}, KBr): $\nu_{C\equiv N}$ 2158, 2136, $\nu_{C=O}$ 1676$_{sh}$, 1654.

The complexes are insoluble in inorganic and organic solvents except water.

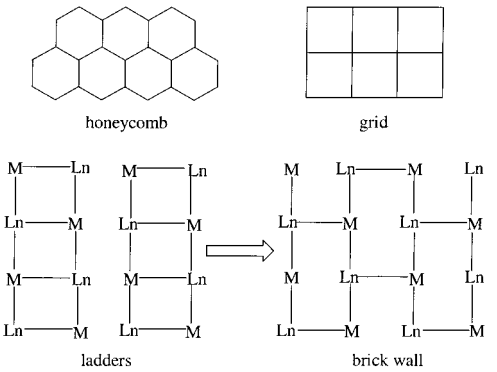

Figure 1. Schematic view of the possible topologies for LnM complexes and transformation of parallel ladders into brick wall.

Crystallographic Data Collection and Structure Determination. The data collections of **2** and **3** were made at 293 K on a Rigaku R-Axis RIPID IP and a Nonius κ-CCD diffractometer, respectively. The structures were solved by the direct method (SHELXS-97) and refined by full-matrix least-squares (SHELEXL-97) on F^2. Anisotropic thermal parameters were used for the non-hydrogen atoms and isotropic parameters for the hydrogen atoms. Hydrogen atoms were added geometrically and refined using a riding model. Weighted R factors (wR) and all of the goodness-of-fit (S) values are based on F^2; conventional R factors (R) are based on F, with F set to zero for negative F^2. The weighting scheme is $w = 1/[s^2F_o^2 + (0.0433P)^2 + 0.0000P]$, where $P = (F_o^2 + 2F_c^2)/3$. The final Fourier map of **3** showed some residual peak and hole in the vicinity of the Sm atom (1.765/−2.051 e Å^{-3}), which is quite normal for complexes containing heavy metals. The crystal data are summarized in Table 1.

Results and Discussion

Synthesis and General Characterization. We have previously reported a cyano-bridged 4f−3d dimer $[Sm(DMF)_4(H_2O)_4Fe(CN)_6]\cdot H_2O$ prepared by the reaction of $Sm(NO_3)_3\cdot 6H_2O$ and $K_3[Fe(CN)_6]$ in a DMF−H_2O mixture. Attempts are being made to synthesize polymeric 4f−3d species with the hope of long-range magnetic ordering. Considering that the polar solvent water has an unfavorable effect on the formation of the network structure,[7] we tried a nonaqueous synthetic procedure or, rather, a reaction with the existence of the least amount of water. When equimolar amounts of $SmCl_3\cdot 6H_2O$ and $(Bu_4N)_3[Cr(CN)_6]$ are mixed in a DMF−MeOH solution at room temperature, a light-yellow solution is obtained. Slow evaporation of the solution results in the isolation of the one-dimensional (1D) chain of the formula $[Sm(DMF)_4(H_2O)_2Cr(CN)_6]\cdot H_2O$ (**2**), as determined by single-crystal X-ray diffraction analysis.

It can be seen that the aforementioned 4f−3d chain and dimers were prepared in an excess of DMF and that there are four coordinated DMF molecules around each lanthanide ion. We infer that a 2D or 3D array might be obtained when fewer bulky DMF molecules, for example, Ln/DMF = 1:2, were employed in the synthesis. Such an LnM array might assume a grid, honeycomb, or brick wall-like topology dependent on the mode of the M−C≡N−Ln linkages (Figure 1). Naturally, a 1D ladder motif might form, as observed in an Eu(II)−Ni(II) complex $[Eu(DMF)_4Ni(CN)_4]_8$.[6c] We found that the reaction between $Sm(NO_3)_3\cdot 6H_2O$, DMF, and $K_3[Cr(CN)_6]$ in the molar ratio of 1:2:1 in H_2O afforded a 2D brick wall-like complex $[Sm(DMF)_2(H_2O)_3Cr(CN)_6]\cdot H_2O$ (**3**).

The IR spectra of the complexes show two sharp bands (2141 and 2126 cm^{-1} for **2** and 2158 and 2136 cm^{-1} for **3**) in the range 2000−2200 cm^{-1} that are attributed to C≡N stretching modes. The splitting of ν(C≡N) suggests the presence of both bridged and nonbridged CN^- ligands. The strong bands at 1653

(9) Kou, H.-Z.; Gao, S.; Sun, B.-W.; Zhang, J. *Chem. Mater*. **2001**, *13*, 1431.
(10) Cruser, F. V. D.; Miller, E. H. *J. Am. Chem. Soc*. **1906**, *28*, 1132.
(11) Mascharak, P. K. *Inorg. Chem*. **1986**, *25*, 245.

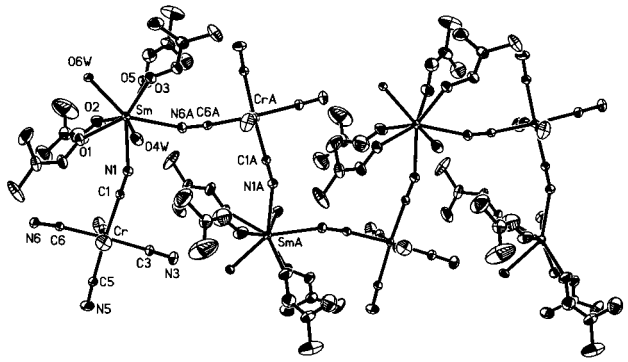

Figure 2. Chainlike structure of **2**.

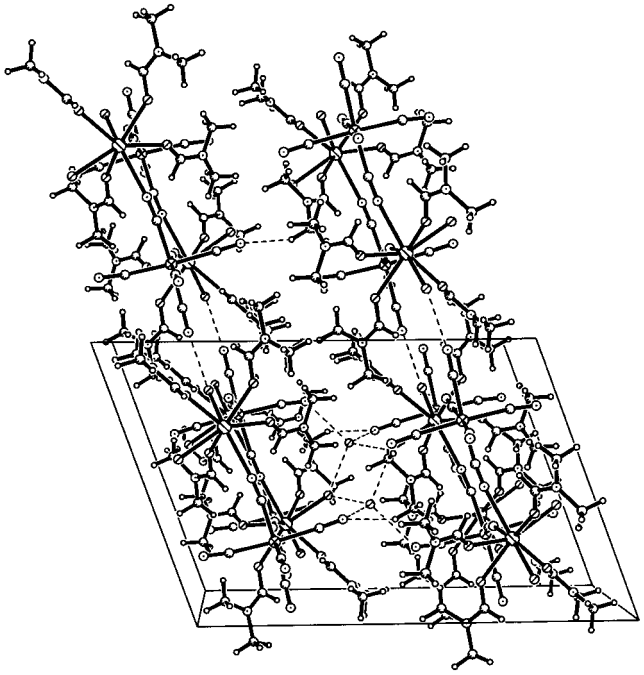

Figure 3. Unit cell packing diagram of **2**, showing the hydrogen-bonded chains.

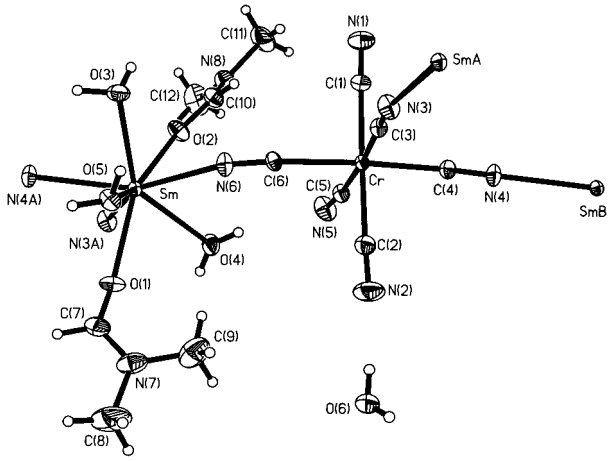

Figure 4. ORTEP plot of **3** with the numbering of the unique atoms.

cm^{-1} for **2** and 1676_{sh} and 1654 cm^{-1} for **3** are assigned to the C═O stretching vibration (DMF).

Crystal Structures. ORTEP drawings of complexes **2** and **3** are shown in Figures 2 and 4, respectively. Figures 3 and 5 show the unit cell packing diagrams of **2** and **3**, respectively. Selected bond distances and angles for **2** and **3** are listed in Tables 2 and 3, respectively.

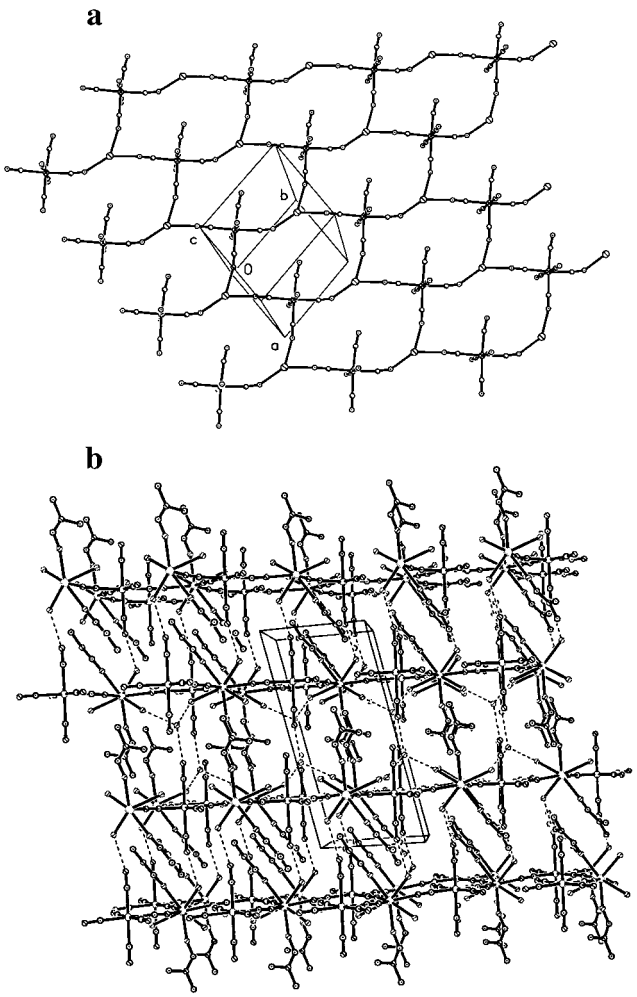

Figure 5. (a) Projection of **3** along the *c* axis showing the brick wall-like backbone (DMF and H_2O molecules are omitted for clarity). (b) Projection of **3** along the *b* axis showing the H-bonded layers.

Table 2. Selected Bond Lengths (Å) and Angles (deg) for **2**[a]

Bond Length (Å)			
Sm−O(1)	2.378(4)	Sm−O(2)	2.386(4)
Sm−O(3)	2.391(3)	Sm−O(4W)	2.438(4)
Sm−O(5)	2.408(4)	Sm−O(6W)	2.374(4)
Sm−N(1)	2.538(4)	Sm−N(6)#1	2.537(4)
Cr−C(1)	2.082(5)	Cr−C(2)	2.067(6)
Cr−C(3)	2.068(5)	Cr−C(4)	2.063(5)
Cr−C(5)	2.077(5)	Cr−C(6)	2.098(5)
C(2)−N(2)	1.149(7)	C(1)−N(1)	1.143(6)
C(3)−N(3)	1.134(7)	C(4)−N(4)	1.145(6)
C(5)−N(5)	1.129(6)	C(1)−N(1)	1.144(6)
Angle (deg)			
N(2)−C(2)−Cr	172.0(5)	N(1)−C(1)−Cr	174.6(4)
N(3)−C(3)−Cr	178.1(5)	N(4)−C(4)−Cr	173.3(5)
N(5)−C(5)−Cr	177.4(5)	N(6)−C(6)−Cr	171.2(4)
C(6)−N(6)−Sm#2	163.0(4)	C(1)−N(1)−Sm	159.4(4)

[a] Symmetry transformations used to generate equivalent atoms: #1, $-x+1, y+{}^1/_2, -z+{}^1/_2$; #2, $-x+1, y-{}^1/_2, -z+{}^1/_2$.

The structure of **2** consists of a cyano-bridged alternating array of $Cr(CN)_6$ and $Sm(DMF)_4(H_2O)_2$ fragments. The Sm atom is eight-coordinated with a distorted square antiprism geometry. Six oxygen atoms of two water molecules and four DMF molecules and two nitrogen atoms of the bridging CN ligands are bound to Sm, with an Sm−O distance ranging from 2.374(4) to 2.438(4) Å. Two bridging cyanides coordinate to the samarium(III) ion [N(1)−Sm = 2.538(4) Å and N(6)−Sm#2 = 2.537(4) Å] in a bent fashion, with bond angles of 159.4(4)°

Table 3. Selected Bond Lengths (Å) and Angles (deg) for **3**[a]

Bond Length (Å)			
Sm−O(1)	2.361(3)	Sm−O(2)	2.345(3)
Sm−O(3)	2.445(4)	Sm−O(4)	2.442(3)
Sm−O(5)	2.447(3)	Sm−N(6)	2.520(4)
Sm−N(4)#1	2.514(4)	Sm−N(3)#2	2.524(4)
Cr−C(1)	2.059(4)	Cr−C(2)	2.074(5)
Cr−C(3)	2.071(4)	Cr−C(4)	2.081(4)
Cr−C(5)	2.072(4)	Cr−C(6)	2.075(4)
C(2)−N(2)	1.138(6)	C(1)−N(1)	1.144(6)
C(3)−N(3)	1.149(5)	C(4)−N(4)	1.129(5)
C(5)−N(5)	1.152(6)	C(1)−N(1)	1.131(5)
Angle (deg)			
N(2)−C(2)−Cr	177.9(4)	N(1)−C(1)−Cr	177.3(5)
N(3)−C(3)−Cr	179.5(4)	N(4)−C(4)−Cr	177.0(4)
N(5)−C(5)−Cr	172.6(4)	N(6)−C(6)−Cr	171.2(4)
C(6)−N(6)−Sm	152.7(3)	C(4)−N(4)−Sm#3	175.0(3)
C(3)−N(3)−Sm#4	167.1(3)		

[a] Symmetry transformations used to generate equivalent atoms: #1, $x-1, y-1, z$; #2, $x, y-1, z$; #3, $x+1, y+1, z$; #4, $x, y+1, z$.

for C(1)−N(1)−Sm and 163.0(4)° for C(6)−N(6)−Sm#2 (#2 denotes the symmetry transformation $-x+1, y-0.5, -z+0.5$). Each $Cr(CN)_6$ coordinates to two Sm(III) ions using two *cis*-cyanide ligands, while each $Sm(DMF)_4(H_2O)_2$ group connects two $Cr(CN)_6$ moieties in a cis fashion, giving rise to a zigzag chainlike structure. The average value of $N-Sm-O_{H_2O}$ angles is 112.14(15)°, larger than that of the average $N-Sm-O_{DMF}$ angles [94.92(15)°]. A similar result is observed in complex **3** and in other cyano-bridged LnM species with both H_2O and DMF in the coordination sphere of Ln.[4−6] This reflects that small water molecules are more polar than bulky DMF and that the electrostatic repulsion force is dominant and decisive. The adjacent intrachain metal−metal distances are 5.660(1), 5.667(1), and 7.326(1) Å for Cr···Sm, Cr···Sm#2, and Cr···Sm#1 (#1: $-x+1, y+0.5, -z+0.5$), respectively. The nearest interchain metal−metal separation is 7.623(1) Å for Cr···Sm#3 (#3: $x+1, y, z$).

The coordinated water molecule, O(4W), is hydrogen-bonded to the lattice water molecule, O(1W), with an O(1W)···O(4W) contact of 2.811(5) Å. In addition, the terminal cyanide ligands are also hydrogen-bonded to the water molecules O(6W) and O(1W), with the O−N separations ranging from 2.772 to 2.897 Å. Therefore, the molecular structure can be described as a hydrogen-bonded 3D network derived from SmCr chains (Figure 3).

Complexes **3** and **1**[9] are isostructural and consist of 2D brick wall-like layers with slightly distorted Cr_3Sm_3 rectangles. Each $[Cr(CN)_6]^{3-}$ unit uses three cyanide groups in the meridional arrangement to connect with three $[Sm(DMF)_2(H_2O)_3]^{3+}$ units, and each $[Sm(DMF)_2(H_2O)_3]^{3+}$ unit, in turn, links with three $[Cr(CN)_6]^{3-}$ (Figure 4). The metal ions within a layer lie in a plane with the largest deviation of 0.17 Å for Sm. This local molecular disposition extends, generating a flat brick wall-like topology. A similar linking mode was observed in the ladder-like complex $[Eu(DMF)_4Ni(CN)_4]_8$.[6c] Actually, the brick wall network can be generated by linking the ladders via the displacement of every other rung of the parallel ladders (Figure 1). The bridging cyanide ligands coordinate to the Sm(III) ions in two different fashions: two nearly linear, [Sm−N(4)#1−C(4)#1 = 175.0(3)° and Sm−N(3)#2−C(3)#2 = 167.1(3)°] and one bent [Sm−N(6)−C(6) = 152.7(3)°] (#1 and #2 denote the symmetry transformations $x-1, y-1, z$ and $x, y-1, z$, respectively), leading to a slight distortion of the brick wall. This observation supports the proposition by Kautz et al. that the Ln−N≡C−M linkage angles are most probably affected by steric factors and crystal packing forces.[5] In complex **3**, the bent Sm−N(6)−C(6) linkage is due to the steric hindrance of the coordinated DMF molecules (Figure 4). The Sm(III) ion exists in a slightly distorted square antiprism coordination geometry with a dihedral angle between the two faces of 2.7(2)°. The Sm−O bond distances range from 2.345(3) to 2.447(3) Å, and the Sm−N bond lengths range from 2.514(4) to 2.524(4) Å. The adjacent Cr···Sm distances are 5.487(1) Å for Cr···Sm, 5.708(1) Å for Cr···Sm#3, and 5.718(1) Å for Cr···Sm#4, respectively (#3, $x, y+1, z$; #4, $x+1, y+1, z$). The shortest interlayer metal−metal distance is 7.743(1) Å for Cr···Sm#5 (#5, $1-x, 1-y, -z$). The unit cell packing diagram (Figure 5) shows four parallel layers. The flat layers align parallel with separations of ca. 7.4(1) and 8.5(1) Å, respectively. The uncoordinated water molecules are positioned between the distantly separated layers and linked to one terminal CN^- ligand of $[Cr(CN)_6]^{3-}$ and the coordinated water molecules via hydrogen bonding. Between the closer layers, the nonbridging cyanide ligands interact with the coordinated water molecules through hydrogen bonds to connect the two layers.

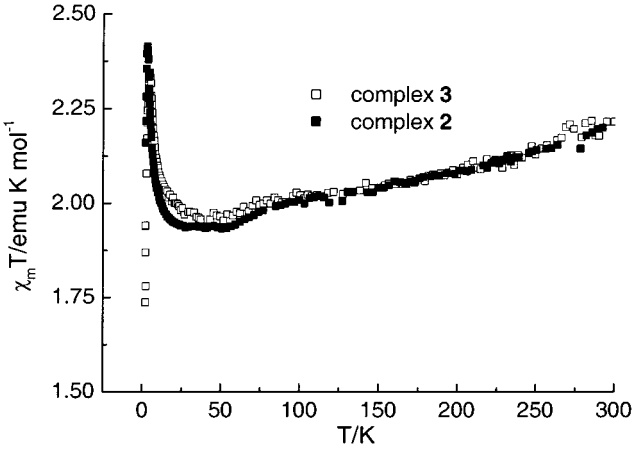

Figure 6. Temperature dependences of $\chi_m T$ in an applied field of 10 kOe for **2** and **3**.

Magnetic Properties. The variable-temperature (2−300 K) magnetic susceptibilities of **2** and **3** have been measured on a bunch of small crystals in a field of 10 kOe. A plot of $\chi_m T$ versus T for **2** and **3** is shown in Figure 6, where χ_m is the magnetic susceptibility per SmCr unit. The $\chi_m T$ value at 300 K is ca. 2.24 emu K mol^{-1} (the calculated value is in the range of 2.16−2.24 emu K mol^{-1} assuming $g_{Cr} = 2.0$),[12] which decreases smoothly with a decrease of the temperature, reaching a minimum value of 2.0 and 1.9 emu K mol^{-1} at 52 and 45 K for **3** and **2**, respectively. With a further decrease of the temperature, $\chi_m T$ increases sharply, reaching a maximum value of 2.4 emu K mol^{-1} at 4.5 K before decreasing again. The magnetic susceptibilities of both of the complexes deviate from the Curie−Weiss law, which is caused by first- and second-order Zeeman effect contributions of the ground ($^6H_{5/2}$) and first excited ($^6H_{7/2}$) states of Sm(III), which are close in energy and thermally populated at room temperature because of the relatively low spin−orbit coupling effect. Therefore, the nature of the magnetic coupling between the adjacent Sm(III) and Cr(III) ions cannot simply be determined from the decrease of $\chi_m T$, which should be due to the superposition of thermal depopulation of the low-lying excited states of Sm(III) and the Sm(III)−Cr(III) magnetic interaction. Hulliger et al. have demonstrated that the Sm(III)−Cr(III) magnetic interaction in

(12) Baker, A. T.; Hamer, A. M.; Livingstone, S. E. *Transition Met. Chem.* **1984**, *9*, 423.

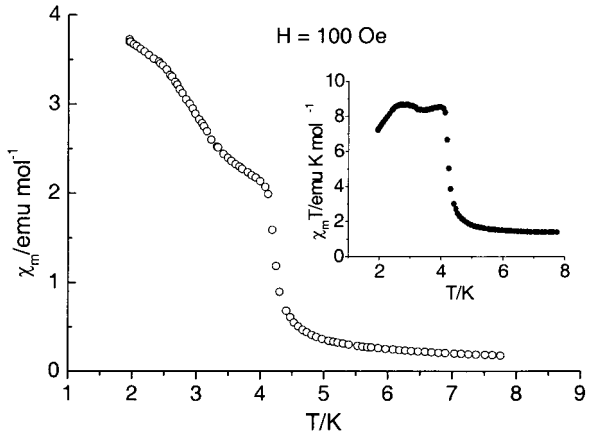

Figure 7. FCM for **3**. Inset: Corresponding $\chi_m T$ product as a function of temperature in a 100 Oe field for **3**.

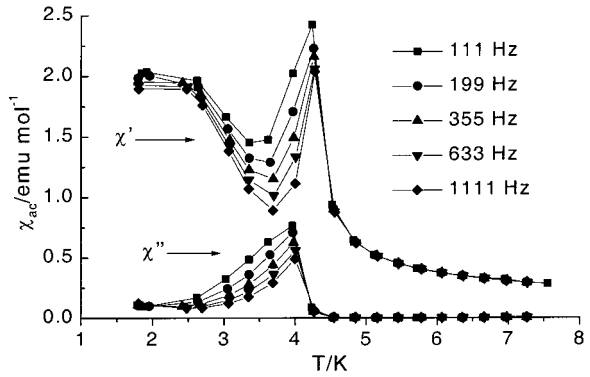

Figure 8. Real (χ') and imaginary (χ'') ac magnetic susceptibilities in zero applied dc field and an ac field of 2 Oe at different frequencies for **3**. The sample was zero-field cooled and data taken upon warming.

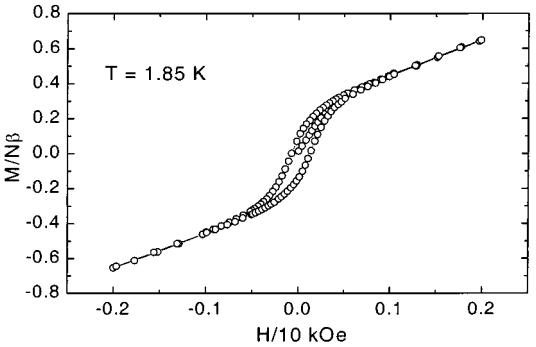

Figure 9. Hysteresis loop at 1.85 K for **3**.

3D $SmCr(CN)_6 \cdot 4H_2O$ is antiferromagnetic.[2] To ascertain the nature of magnetic coupling between magnetic-lanthanide and transition-metal ions, an experimental methodology has been developed in which the intrinsic rare-earth ion magnetic properties are dismissed by comparing the $\chi_m T$ versus T curves for two isostructural analogues [i.e., LnM and LnM′ where M and M′ represent a paramagnetic and a diamagnetic transition-metal ion, respectively (for example, Cu^{2+} and Zn^{2+})]. The difference of the $\chi_m T$ products of these two species, for a given lanthanide ion, affords information about the nature of the magnetic interaction between Ln(III) and paramagnetic M(II) ions.[7,13,14] In our experiment, we were not able to synthesize SmCo analogues of complexes **3** and **2**; therefore, such an approach could not be used.

The FCM curve of **3** measured in a low field of 100 Oe shows an abrupt increase in χ_m at ca. 4.2 K (Figure 7). The absence of a peak down to 2.0 K suggests long-range magnetic ordering due to the ferromagnetic interaction between the adjacent layers. The derivative curve (dFCM/dT) presents an extremum at 4.2 K, corresponding to the transition temperature (T_c). The corresponding $\chi_m T$ product as a function of temperature for **3**, shown in the inset of Figure 7, presents two maximums at 2.7 and 3.9 K, suggesting the existence of two transitions. This is evidenced by the ac magnetic susceptibility measurements.

The temperature dependence of ac magnetic susceptibilities for complex **3** verifies the magnetic-phase transition temperature at 4.2 K defined by the inflection point in χ' as well as the point where distinct χ'' appears (Figure 8). This ordering temperature is in good agreement with that of the FCM result. Below T_c, the frequency dependence of ac magnetic susceptibilities suggests the presence of a degree of spin-glass behavior, and the increase of χ' below 3.5 K indicates an unidentified transition, which may be tentatively attributed as a reentrant spin-glass state.[15]

The field dependence of the magnetization (0−70 kOe) for complex **3**, measured at 1.8 and 3.0 K, shows a rapid saturation of magnetization, as expected for a magnet. The saturation magnetization reaches a value of 3.5 Nβ at 1.8 K, higher than the literature value of 2.2 Nβ for the 3D SmCr ferrimagnet.[2] A hysteresis loop at 1.85 K (Figure 9) for complex **3** is observed with a coercive field of 100 Oe, larger than that of the GdCr analogue **1** (less than 10 Oe).[9] This indicates that the coercive field might be tuned by the choice of lanthanide ions with large magnetic anisotropy. It is worth mentioning that the structure parameters of **3** are very close to that of isostructural complex **1**. However, different bulky magnetic properties are observed: ferromagnetic-like ordering for **3** and antiferromagnetic ordering for **1**. This suggests that the nature of the intra- and interlayer magnetic interactions relate to the interacting metal ions. The ferromagnetic-like behavior of **3** might be from the stronger magnetic anisotropy of Sm compared with that of Gd in **1**.

The temperature dependence of zero-static field ac magnetic susceptibilities for complex **2** shows that the in-phase component (χ') has no maximum down to 2.0 K for frequencies of 199, 355, 633, and 1111 Hz and that the out-of-phase component (χ'') remains at zero, indicating that no magnetic ordering occurs down to 2.0 K. This reveals that the interchain magnetic interaction through H bonds in 1D species usually results in lower or no magnetic-phase transition temperature. The field dependence of the magnetization (0−70 kOe) for complex **2** measured at 1.8 and 4.2 K shows the saturation of magnetization reaching a value of 3.1 (2.9) Nβ at 2.0 (4.2) K, close to that for complex **3** and higher than the literature value of 2.2 Nβ for $SmCr(CN)_6 \cdot 4H_2O$.[2] On the basis of the present results, it follows that the magnetic exchange between adjacent Sm(III)···Cr(III) is ferromagnetic-like rather than antiferromagnetic. Therefore, the decrease in $\chi_m T$ for complexes **2** and **3** should be due to the dominant thermal depopulation of the low-lying excited states of Sm(III) to which Sm(III)−Cr(III) ferromagnetic coupling is superimposed. Obviously, this supposition should be supported by further experimental results, for example, by comparison of magnetic properties for isostructural Sm(III)−Cr(III) and Sm(III)−Co(III) complexes. Further work along this line is in progress in our group.

(13) Kahn, M. L.; Mathoniere, C.; Kahn, O. *Inorg. Chem.* **1999**, *38*, 3692.
(14) Kahn, M. L.; Lecante, P.; Verelst, M.; Mathoniere, C.; Kahn, O. *Chem. Mater.* **2000**, *12*, 3073.
(15) Wasiutynski, T.; Szeglowski, Z.; Pacyna, A. W.; Balanda, M. *Physica B* **1998**, *253*, 305.

Conclusion

We have synthesized a new cyano-bridged 2D brick wall-like lanthanide transition-metal complex (**3**) exhibiting long-range magnetic ordering at 4.2 K and a new cyano-bridged 1D zigzag chainlike complex (**2**). The absence of magnetic ordering down to 2.0 K for complex **2** is in part due to the weak interchain magnetic interaction propagated through hydrogen bonds. In contrast to the 3D parent complex, the low critical temperature of the 2D complex (**3**) is connected with the weak interlayer magnetic interaction in a 2D system. Therefore, the synthesis of new cyano-bridged 3D 4f−3d arrays is our next target.

Acknowledgment. This work was supported by the State Key Project of Fundamental Research (Grant G1998061305), the National Natural Science Foundation of China (Grants 20023005 and 29831010), the Postdoctoral Science Foundation of China, and the Excellent Young Teachers Fund of MOE, P. R. China.

Supporting Information Available: An X-ray crystallographic file (CIF). Field dependence (0−70 kOe) of magnetization for **3** and **2**. This material is available free of charge via the Internet at http://pubs.acs.org.

IC0103042